

# Exploring Structural Features of the Interaction Between the Scorpion Toxin CnErg1 and *ERG* K<sup>+</sup> Channels

Karine Fréchal,<sup>1†</sup> Chen-Qi Xu,<sup>2,4†</sup> Nicolas Wolff,<sup>1</sup> Karine Wecker,<sup>1</sup> Georgina B. Gurrola,<sup>3</sup> Shun-Yi Zhu,<sup>4</sup> Cheng-Wu Chi,<sup>2,5</sup> Lourival D. Possani,<sup>3</sup> Jan Tytgat,<sup>4\*</sup> and Muriel Delepierre<sup>1\*</sup>

<sup>1</sup>Unité de RMN des Biomolécules URA 2185 CNRS, Institut Pasteur, Paris, France

<sup>2</sup>Key Laboratory of Proteomics, Institute of Biochemistry and Cell Biology, Chinese Academy of Sciences, Shanghai, China

<sup>3</sup>Department of Molecular Medicine and Bioprocesses, Institute of Biotechnology, National Autonomous University of Mexico, Cuernavaca, Mexico

<sup>4</sup>Laboratory of Toxicology, University of Leuven, Leuven, Belgium

<sup>5</sup>Institute of Protein Research, Tong Ji University, Shanghai, China

**ABSTRACT** The  $\gamma$ -KTx-type scorpion toxins specific for K<sup>+</sup> channels were found to interact with *ERG* channels on the turret region, while  $\alpha$ -KTx3.2 Agitoxin-2 binds to the pore region of the *Shaker* K<sup>+</sup> channel, and  $\alpha$ -KTx5.3 BmP05 binds to the intermediate region of the small-conductance calcium-activated K-channel (SK<sub>Ca</sub>). In order to explore the critical residues for  $\gamma$ -KTx binding, we determined the NMR structure of native  $\gamma$ -KTx1.1 (CnErg1), a 42 amino acid residues scorpion toxin isolated from the venom of the Mexican scorpion *Centruroides noxius* Hoffmann, and we used computational evolutionary trace (ET) analysis to predict possible structural and functional features of interacting surfaces. The <sup>1</sup>H-NMR three-dimensional solution structure of native ergtoxin (CnErg1) was solved using a total of 452 distance constraints, 13 <sup>3</sup>J<sub>NH-H $\alpha$</sub>  and 10 hydrogen bonds. The structure is characterized by 2 segments of  $\alpha$ -helices and a triple-stranded antiparallel  $\beta$ -sheet stabilized by 4 disulfide bridges. The ET and structural analysis provided indication of the presence of two important amino acid residue clusters, one hydrophobic and the other hydrophilic, that should be involved in the surface contact between the toxin and the channel. Some features of the proposed interacting surface are discussed. *Proteins* 2004;56:367–375. © 2004 Wiley-Liss, Inc.

**Key words:** *ERG* channel; ergtoxin; evolutionary trace analysis; NMR structure; scorpion toxin

## INTRODUCTION

K<sup>+</sup> channels play critical roles in a wide variety of physiological processes, including the regulation of heart rate, muscle contraction, neurotransmitter release, and cell proliferation.<sup>1</sup> K<sup>+</sup> channels are a diverse superfamily of more than 80 members. For the purpose of hunting and defense, during the process of evolution, scorpions have been able to select many different bioactive peptides, among which are toxins capable of blocking the function of K<sup>+</sup> channels. So far, more than 100 different K<sup>+</sup> channel toxins have been found from scorpion venoms.<sup>2,3</sup> According to their primary structures and functions, they have

been classified into three subfamilies called  $\alpha$ -,  $\beta$ -, and  $\gamma$ -KTx's.<sup>2</sup>  $\alpha$ -KTx is the largest family containing more than 80 members active on Kv, BK<sub>Ca</sub>, or SK<sub>Ca</sub> channels. They are short-chain toxins with 23–41 amino acids containing 3 or 4 disulfide bridges.  $\beta$ -KTx's are long-chain toxins composed of 60–64 amino acids but containing only 3 disulfide bridges.  $\gamma$ -KTx's are *hERG* channel blockers with 36–47 amino acids containing 3 or 4 disulfide bridges.

The *hERG* channel, a product of the human *ether-à-go-go*-related (*erg*) gene,<sup>4</sup> is mostly expressed in the heart, where it plays a crucial role in the repolarization phase of the cardiac action potential. Mutations on this channel are responsible for the inherited long QT syndrome (LQT) that may cause syncope and sudden death resulting from arrhythmias and ventricular fibrillation.<sup>5</sup> A number of *hERG*-blocking drugs have also been shown to cause acquired LQT and an increased risk of sudden death.<sup>1</sup> Thus, it is worth fully studying the interaction mode between this channel and its ligands. Recently, mutagenesis work was performed on the *hERG* channel to figure out the binding sites of scorpion  $\gamma$ -KTx1.1, CnErg1.<sup>6</sup> The results indicate that CnErg1 can bind to the external amphipathic  $\alpha$ -helix of the *hERG* channel, but not to the central pore region, as opposed to most other Kv blockers. This means that scorpion  $\gamma$ -KTx might adopt a novel interaction mode to block the *hERG* channel, which is completely different from the two other interaction modes in which AgTx2 binds to the internal region of *Shaker* and P05 binds to the intermediate region of the SK<sub>Ca</sub> channel.<sup>3,7</sup> Consequently, this novel mode of interaction raises the question: Which are the crucial residues in CnErg1 involved in this interaction?

<sup>†</sup>These authors contributed equally to the work.

Grant sponsor: Mexican Council of Science and Technology (CONACYT); Grant number: 40251-Q (to L. Possani).

\*Correspondence to: Jan Tytgat, Laboratory of Toxicology, University of Leuven, 3000 Leuven, Belgium. E-mail: jan.tytgat@pharm.kuleuven.ac.be; and Muriel Delepierre, Unité de RMN des Biomolécules URA 2185 CNRS, Institut Pasteur, 28 Rue du Dr Roux, 75 724 Paris cedex 15, France. E-mail: muriel@pasteur.fr

Received 25 September 2003; Accepted 5 January 2004

Published online 2 April 2004 in Wiley InterScience (www.interscience.wiley.com). DOI: 10.1002/prot.20102

To answer this question, the structure of the native  $\gamma$ -KTx1.1 was determined in solution, and a computational evolutionary trace (ET) analysis method was applied to study the structural and functional evolution of scorpion  $\gamma$ -KTx and  $\alpha$ -KTx.<sup>8</sup> Using <sup>1</sup>H NMR data obtained from a limited amount of native CnErg1, we have elucidated the three-dimensional (3D) structure of the native toxin. This was rendered possible with the simultaneous use of NMR technology for working with small amounts of compound and the molecular modelization approach using Discover and ARIA modelization programs in a complementary fashion. Whereas, during the process of this work, the NMR structure of a chemically synthesized CnErg1 was published,<sup>9</sup> we present here the first structure of the native CnErg1. As stated before, we have additionally used an ET analysis and applied the obtained results on the 3D structure of CnErg1 to highlight its functional sites.

ET uses phylogenetic information to rank the residues in a protein sequence by evolutionary importance. This method has now been used by many investigators to identify protein functional sites and to study protein-protein docking.<sup>10–12</sup> To date, ET results could always be confirmed by mutagenesis studies.<sup>8</sup> Considering that CnErg1 showed very high sequence homology with other  $\gamma$ -KTx's, this toxin was the focus of this work. ET highlighted two patches of CnErg1, located opposite each other, which may be directly involved in toxin binding.

## MATERIALS AND METHODS

### Evolutionary Trace Analysis

Scorpion short-chain toxins affecting K<sup>+</sup> channels, including 88  $\alpha$ -KTx's and 27  $\gamma$ -KTx's to date, were obtained from the GenBank database.  $\beta$ -KTx's were excluded, because they are long-chain toxins. These 88  $\alpha$ -KTx's have been classified into 18 subfamilies, and 27  $\gamma$ -KTx's have been classified into 5 subfamilies.<sup>2,3</sup> Considering that the sequence homology among toxins from the same subfamily is quite high, we chose two sequences from every subfamily to represent the whole subfamily members, while some subfamilies that are putative K<sup>+</sup> channel blockers were not chosen. Finally, 41 sequences were used to do ET analysis. Multiple sequence alignment was performed by using the program ClustalX and then refined manually. The ET analysis was then carried out on the Evolutionary Trace Server (TraceSuite II) developed by the University of Cambridge.<sup>11–13</sup> First, a phylogenetic tree based on a measure of sequence resemblance was constructed. Gap was treated as a 21<sup>st</sup> residue. Partition identity cutoffs (PICs) were defined as boundaries that partition the tree into clusters at certain values of percentage sequence identity (Fig. 1). Within the same cluster, its members were comparable with regard to sequence and function. For each cluster, a consensus sequence was constructed, and the consensus sequences of each cluster were combined together to produce an ET sequence.<sup>10</sup> All residues were divided into three classes: neutral, conserved, and class-specific. If the residues in a given position were identical in all the consensus sequences, this position was classified as conserved and shown in the ET sequence. If any one or more of the original consensus sequences were blank

at a given position, then that position was classified as neutral and left blank in the ET sequence. If the original consensus sequences all highlighted a given position, but the position showed variation between the consensus sequences, then that position in the ET sequence was classified as class-specific and given the symbol X. The class-specific residues were the most important residues for the functional diversity of different clusters.

## NMR Structure Determination

### Sample preparation

CnErg1 was isolated from the venom of the Mexican scorpion *Centruroides noxius* Hoffmann.<sup>14</sup> Its amino acid sequence was obtained by direct Edman degradation,<sup>15</sup> and its 4 disulfide bridges (Cys5-Cys23, Cys11-Cys34, Cys20-Cys39, and Cys24-Cys41) were determined by mass spectrometry after digestion with trypsin. Native CnErg1, about 400  $\mu$ g of lyophilized powder, was dissolved first in 40  $\mu$ L of H<sub>2</sub>O/D<sub>2</sub>O, 9:1 (v/v) (Eurisotop). The sample concentration was at most 1.4 mM, but probably less, and the pH of the solution was about 3. We have to emphasize here that it is always difficult to control both the exact concentration and the pH when quantities are so scarce. Then, 150  $\mu$ g of lyophilized CnErg1 was added, and the volume was completed to 160  $\mu$ L with H<sub>2</sub>O/D<sub>2</sub>O, 9:1 for experiments in a 3 mm Shigemi tube.

### NMR experiments

A first series of <sup>1</sup>H NMR experiments were performed at 303 and 313 K on a 500 MHz Varian Inova spectrometer (equipped with a Sun Sparc Ultra 2 station and the VNMR 6.1 software), using a nano-nmr probe (Varian) of 40  $\mu$ L. The sample was spun at magic angle at a rate of 2500 Hz. Adiabatic total correlated spectroscopy (TOCSY),<sup>16</sup> nuclear Overhauser effect spectroscopy (NOESY),<sup>17</sup> correlated spectroscopy (COSY),<sup>18</sup> and double-quantum correlated spectroscopy (DQ-COSY)<sup>19</sup> were recorded.

A second series of <sup>1</sup>H NMR experiments were performed using a 3 mm Shigemi tube and 160  $\mu$ L of sample. These experiments were run at 288 K on the 500 MHz spectrometer and at 276, 283, and 303 K on a 600 MHz Varian Inova spectrometer (equipped with a Sun Sparc Ultra 5 station and the VNMR 6.1 software). This allows us to improve the signal to noise, as the field is higher in particular for the NOESY experiment, which for a yet unknown reason is less sensitive with the nanoprobe, although the concentration is higher. TOCSY<sup>20</sup> (80 ms mixing time, 96 scans) and NOESY (250 ms mixing time, 128 scans) experiments using a WATERGATE sequence<sup>21</sup> to suppress the water signal were recorded at each temperature.

Proton chemical shifts were given relative to the 2,2-dimethyl-2-silapentane-5-sulfonic acid (DSS). All the spectra were recorded with 1024  $\times$  2048 points except for the COSY spectrum recorded with 1024  $\times$  8192 points. Zero filling was applied in the two dimensions.

### Proton resonance frequency assignment

Identification of spin systems was obtained by the analysis of the purged COSY, DQ-COSY, TOCSY, and

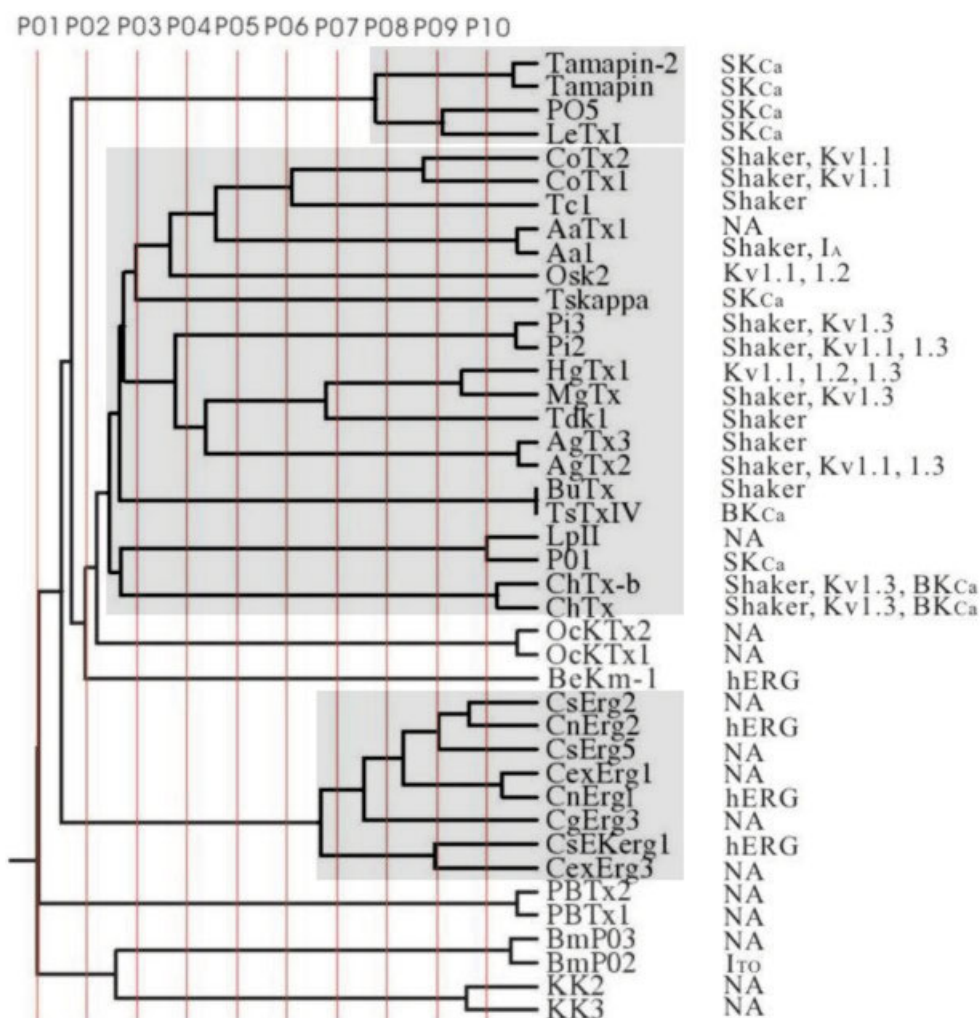


Fig. 1. Phylogenetic tree constructed from the 41 sequences of scorpion  $\alpha$ -KTx and  $\gamma$ -KTx. Partition identity cutoffs (PIC) P01–P10 are shown as thin vertical lines. The members clustered together with the similar function are shadowed. Main biotargets of every toxin are listed here (NA, not available).

NOESY spectra at different temperatures. A NOESY experiment was recorded in D<sub>2</sub>O to identify the aromatic ring protons of the 3 tyrosines and the 2 phenylalanines, as well as interactions between the H $\alpha$  protons in the  $\beta$ -sheet.

CnErg1 sequence-specific assignment was achieved according to the standard method developed by Wüthrich.<sup>22</sup> Using different temperatures helped in solving ambiguities due to many overlapping resonances. Several starting points were used for assignment: the two unique spin systems, Val6 and Thr33, and then the identified Ala, Gly, and Ser from their characteristic spin systems. The sequential assignment was obtained using the connectivities NH<sub>i</sub>-NH<sub>i+1</sub>, H $\alpha_i$ -NH<sub>i+1</sub>, and H $\beta_i$ -NH<sub>i+1</sub> observed in the NOESY spectra recorded with a 250 ms mixing time in H<sub>2</sub>O and processed with VNMR (Varian, Inc.) and analysed with XEASY.<sup>23</sup> All spin systems, except the Asp1, were thus identified (Table I in supplementary material).

### Experimental restraints

Distance constraints were obtained from the NOESY spectra recorded in H<sub>2</sub>O and D<sub>2</sub>O at 303 K, with a 250 ms

mixing time (Fig. 2). Additional distance constraints for structure calculations using DISCOVER/NMRchitect were obtained from NOESY recorded at 278 K and 283 K in H<sub>2</sub>O. <sup>3</sup>J<sub>NH-H $\alpha$</sub>  coupling constants were estimated from the COSY spectrum at 303 K, with a digital resolution of 0.75 Hz per point.

For amide proton–deuterium exchange measurements, the sample was lyophilized and the powder was dissolved in 160  $\mu$ L of pure D<sub>2</sub>O. One-dimensional spectra were acquired at 600 MHz, and 303 K, 30 min, 1h, 1h10, 1h20, and 1h40 after D<sub>2</sub>O addition. Main-chain amide proton temperature coefficients were calculated from chemical shifts determined at 276, 283, 288, and 303 K.

### Nuclear Overhauser effect (NOE) assignments and structure calculations

CnErg 1 structure was elucidated, starting with the same list of constraints, using both the ARIA/CNS (Crystallography & NMR System) program and the Discover/NMRchitect package. However, using ARIA allowed us to first treat the ambiguous restraints and to confirm manual

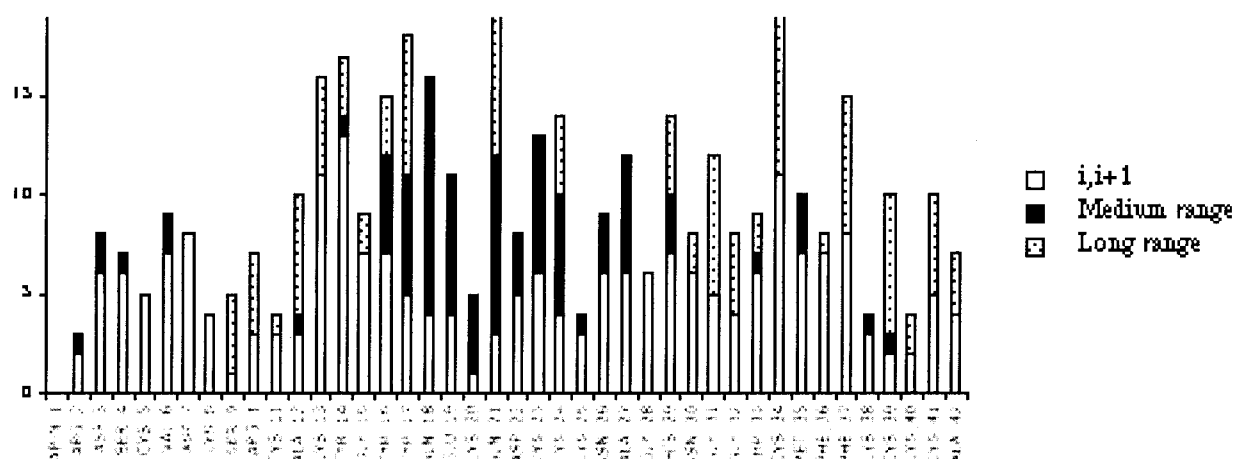


Fig. 2. Distribution of NOE distance restraints by residue used in the structure calculation of CnErg1. The distances have been classified into 3 categories ( $i, i+1$ ), medium range, and long range.

assignments, and second, to overcome long-range NOE assignment ambiguities, leading to an internal and independent check of data. This was rendered compulsory by the paucity of the restraints linked to the low sample concentration. At the final stage, the number of restraints used in structure calculation with ARIA was slightly less than the number of restraints used in structure calculation with Discover.

**ARIA/CNS.** Peaks from NOESY experiments in  $H_2O$  and  $D_2O$  were assigned by automated method using ARIA 1.2.<sup>24,25</sup> Structures were calculated from data obtained at 303 K, using NOE-derived distance constraints,  $\phi$  angle constraints issued from  $^3J_{NH-H\alpha}$  coupling constants, and putative hydrogen bonds. Hydrogen-bond constraints were used in agreement with exchange measured in  $D_2O$  spectra and with amide temperature coefficients ( $< -4$  ppb/K). Structures were calculated with CNS 1.1.<sup>26</sup> Structure calculations were based on the use of ambiguous distance restraints and floating assignments for prochiral groups. Standard protocols of ARIA were performed using a chemical shift tolerance of 0.02 ppm in each dimension, and structures were calculated with the disulfide arrangement determined by mass spectrometry after digestion of the toxin. Basically, a standard simulated annealing was used for ARIA calculations, with an initial temperature for torsion angle dynamics (TAD) of 10,000 K, a final temperature of 1000 K after the first cooling steps, and of 50 K after the second cooling step. Initially 20,000 steps of molecular dynamics (MD) were run, followed by 8000 MD steps for refinement. In ARIA/CNS structure calculation, 10 restraints leading to systematic violations higher than 0.5 Å and resulting mainly from proton diffusion phenomena among aromatic protons were rejected. One thousand structures were obtained in the last iteration of ARIA, and 100 structures with the lowest total energy were minimized in an explicit-water box using the PARALLHDG 5.3 force field.<sup>27</sup>

**DISCOVER/NMRchitect.** NOE cross-peak intensities obtained from manual assignment were converted into distances by an  $r^{-6}$  dependency and calibrated with respect to a distance average (1.78 Å) deduced from a set of

cysteines geminal  $\beta$  protons, namely, Cys34 and Cys41. Pseudoatom corrections were added for the upper limit involving pseudoatoms for methylene, methyl, or aromatic groups.<sup>22</sup> A total of 452 distance constraints, 13  $\phi$  angles, and 10 hydrogen bonds derived from NMR experiments were used as input for the structure calculations.

The calculations were performed with the DISCOVER/NMRchitect software package from Accelrys Technologies, with AMBER force field using a dielectric constant  $\epsilon = 4^*r$  in order to reduce *in vacuo* electrostatic effects. Structures were generated using a three-stage protocol: (1) Minimization of the linear protein with disulfide bridges was realized using 1000 steps of steepest descents followed by 1000 steps of conjugate gradients, in order to fold the toxin before simulated annealing; (2) restrained dynamical simulated annealing protocol consisted of heating the system to 1000 K for 1 ps and in decreasing the temperature to a final temperature of 300 K in 4 steps of 2, 1.7, 5, and 5 ps, respectively; (3) energy minimization using a Lennard-Jones nonbonded term, under distance restraints, by steepest descent and conjugate gradients, until the maximum derivated value is less than 0.001 kcal/mol/Å. The 10 best energy-minimized structures with the lowest total energy, the lowest distance violations, and the lowest root-mean-square deviation (RMSD) with respect to the backbone were used for final structural analysis.

### Homology modeling

The 3D structure of the *hERG* channel was modeled based on the crystal structure of the KvAP channel, which is the first crystalized voltage-gated  $K^+$  channel.<sup>28</sup> The sequences of *hERG* and KvAP were aligned by Multiple Sequence Alignment Software (ClustalX) and then refined manually. The alignment file was directly submitted to the Swiss-Model server for modeling.<sup>29</sup> Energy minimization (Gromos96) and simulated annealing cycles were run. Swiss-Model computes a confidence factor for each atom in the model of structure, taking into account the deviation of the model from the template structure and the distance trap value used for framework building.

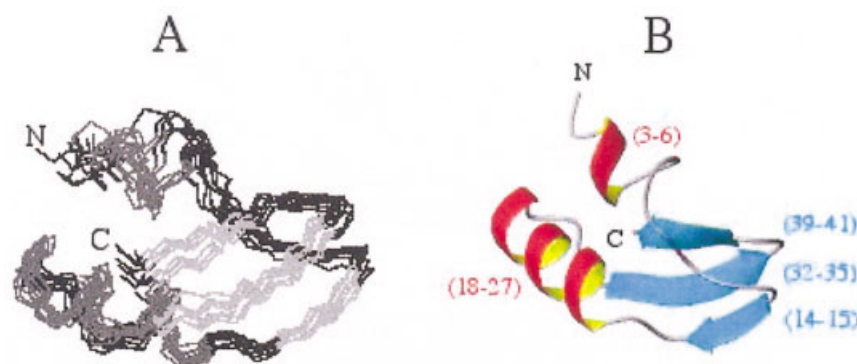


Fig. 3. (A) Backbone superposition of the 10 selected structures of CnErg1. (B) Ribbon view showing the two  $\alpha$ -helices in red (3–6, 18–27) and the triple-stranded antiparallel  $\beta$ -sheet in blue (14–15, 32–35, 39–41).

## RESULTS AND DISCUSSION

### NMR Structure of Native $\gamma$ -KTx1.1, CnErg1 Structure description

The structure of CnErg1 resulting from the Discover procedure (Fig. 3) was obtained by a simulated annealing protocol and energy minimization using 10 hydrogen bonds, 13  $\phi$  angles, and 452 distances constraints, including 252 intraresidual, 108 sequential ( $|i - j| = 1$ ), 43 short-range ( $1 < |i - j| \leq 4$ ) and 49 long-range ( $|i - j| > 4$ ). The final structure set allows several structured regions to be identified with average RMSD of 1.55 Å (residues 2–42) calculated on the backbone atoms (N, C $\alpha$ , C, O). Based on the lowest total energy and the lowest number of NOE restraint violations, 10 structures [Fig. 3(A)] were selected for structural analysis (Table I). This set of structures was compared to those obtained from ARIA/CNS calculations. Similar secondary elements and 3D fold were obtained with an RMSD of 2.33 Å (residues 1–42) calculated on the backbone atoms (N, C $\alpha$ , C, O) between averaged structures obtained from ARIA and Discover calculations.

The structure of the toxin is characterized by an N-terminal sequence poorly organized, extending from Asp1 to Lys13, and including a well-defined short helical fragment from Asp3 to Val 6, upstream from the first  $\beta$ -strand (Tyr14–Tyr15) [Fig. 3(B)]. Then these elements are followed by a 10 amino acid  $\alpha$ -helix encompassing Gln18 to Ala27 residues, the second  $\beta$ -strand (Gly32–Met35), and the third small  $\beta$ -strand extending from Cys39 to Cys41. The N-terminal part is less defined despite the two disulfide bridges (Cys5–Cys23 and Cys11–Cys34) connecting the N-terminal region to the central helix and to the second  $\beta$ -strand. Indeed, only few long-range NOEs are available to connect the N-terminal to the  $\alpha/\beta$  scaffold. CnErg1 adopts then an  $\alpha/\beta$  molecular scaffold localized in (14–41) region, with a conformation of the backbone well defined, corresponding to an RMSD of 0.81 Å (N, C $\alpha$ , C, O). The triple-stranded antiparallel  $\beta$ -sheet is stabilized by 5 hydrogen bonds, namely, HN15–O34, HN33–O40, HN35–O38, HN38–O35, HN40–O33. Observation of five  $^3J_{\text{NH},\text{H}\alpha}$  coupling constants higher than 9 Hz (for Thr33, Cys34, Phe36, Lys38, and Lys40), and several characteristic NOEs such as H $\alpha$ –H $\alpha$  interactions (Gly32–Cys41, Cys34–

TABLE I. Structural Statistics for the Ensemble of 10 Best Final Structures Calculated for (1–42) CnErg1 Obtained by Simulated Annealing

Quantity	Value
Distance restraints	
Intraresidual NOE distance restraints	252
Inter-residual NOE distance restraints	200
( $i, i+1$ )	108
( $i, i+2$ )	17
( $i, i+3$ )	22
( $i, i+4$ )	4
Long range	49
Total	452
Hydrogen bonds restraints ( $^3J_{\text{HN},\text{H}\alpha}$ )	10
Dihedrals angle restraints ( $\phi$ )	13
Total of restraints introduced in the simulated annealing	474
Average of the pairwise RMSDs (Å) of the backbone atoms (N, C $\alpha$ , C, O)	
Residues (1–42)	1.55 $\pm$ 0.48
Residues (3–41)	1.26 $\pm$ 0.33
Residues (14–41)	0.81 $\pm$ 0.26
Residues (3–6, 14–15, 18–27, 32–35, 39–41)	1.20 $\pm$ 0.36
Residual NOE distance constraints violations (Å, 473 constraints)	0.017 $\pm$ 0.002
Residual $^3J_{\text{HN},\text{H}\alpha}$ constraints violations (deg, 10 constraints)	1.07 $\pm$ 0.55
Residual bond distortions (Å, 641 bonds)	0.003 $\pm$ 0.016
Residual angle distortion (deg, 1154 angles)	0.96 $\pm$ 0.42
Conformational energy	
Total (kcal/mol)	–177 $\pm$ 60
Non-bond (kcal/mol)	–139 $\pm$ 17
Restraint energy (kcal/mol)	13 $\pm$ 10

Cys39) confirm the presence of the  $\beta$ -sheet. The well-defined  $\alpha$ -helix (RMSD of 0.60 Å on main-chain atoms) localized between the first and the second  $\beta$ -strand is stabilized by 4 hydrogen bonds (HN23–O19, HN25–O21, HN27–O23, and HN28–O24) and is corroborated by characteristic medium-range NOE cross-peaks: H $\alpha_i$ –NH $_{i+3}$  (19–22, 21–24, 24–27), H $\alpha_i$ –NH $_{i+4}$  (18–22, 19–23, 23–27), and H $\alpha_i$ –H $\beta_{i+3}$  (18–21, 19–22, 20–23, 21–24, 23–26, 24–27).

Since the CnErg1 global fold is quite similar to cysteine-stabilized  $\alpha/\beta$  fold typical of short scorpion toxins, the turn

of helix observed in the N-terminal part of the molecule is one of the new features for this family of molecule. The presence of both 3 positive and 3 negative residues in the N-terminal part of the molecule is also quite new for these potassium channel toxins; moreover, these residues seem to be highly conserved in the  $\gamma$ -KTx subfamily.<sup>30</sup>

### Evolutionary trace analysis

In the TraceSuite server, a rooted phylogenetic tree was built first. In this tree, toxins affecting different targets were mainly clustered into 3 branches: SK<sub>Ca</sub> blockers; *Shaker* (Kv1.X)/BK<sub>Ca</sub> blockers; *hERG* blockers (Fig. 1). BeKm-1, a *hERG* blocker, but having primary structure similar to  $\alpha$ -KTx, took an intermediate position between *hERG* blockers and *Shaker*/BK<sub>Ca</sub> blockers.<sup>31</sup> In *hERG* blocker branches, the functional data of some toxins are not available yet. However, according to their high sequence homology with other neighbors, they should act on the same target. TsKappa and P01, two SK<sub>Ca</sub> blockers with low affinity,<sup>32</sup> were clustered into the *Shaker*/BK<sub>Ca</sub> blockers branch, which implies that they might have other biotargets to be discovered.

As detailed in the Materials and Methods section, PICs, from P01 to P10, were performed (Fig. 1) and all residues were divided into 3 classes in ET sequences: neutral, conserved, and class-specific (Fig. 4). From P01 to P10, only 6 positions occupied by Cys residues were defined as conserved, which can explain that all these toxins probably have the same cysteine-stabilized  $\alpha/\beta$  (CS- $\alpha/\beta$ ) scaffold,<sup>3</sup> as observed for  $\alpha$ -KTx. At P02 PIC, the first class-specific residue Y14 emerged in *hERG* blockers, while it was blank in all other toxins. This residue was well solvent-exposed on the  $\beta$ -sheet 1 together with Y15 between  $\alpha$ -helix 1 and  $\beta$ -sheet 1, and formed a strong hydrophobic patch together with other residues (e.g., F36), which was predicted by Torres et al.<sup>9</sup> to contribute significantly to toxin binding. At P03 PIC, 2 class-specific residues emerged at position 36 and 39. In *Shaker*/BK<sub>Ca</sub> and SK<sub>Ca</sub> blockers, position 36 was completely conserved to be Lys. All the available results of *Shaker* blockers suggest that this Lys residue (equivalent to K27 in ChTX) directly plugs the channel selectivity filter to fully occlude K<sup>+</sup> pathway.<sup>33,34</sup> However, position 36 in *hERG* blockers is occupied by the uncharged residue Thr, explaining the absence of *Shaker* block activity in these toxins. Position 39, located on the  $\beta$ -turn, displays a clear difference in the substitution pattern corresponding to the different pharmacological groups. Indeed, in the highly selective SK<sub>Ca</sub> or BK<sub>Ca</sub> blockers, this position is occupied by the smallest residue Gly, while in the highly selective *Shaker* blockers and some toxins blocking both *Shaker* and BK<sub>Ca</sub>, the position is occupied by one large polar residue Asn. In *hERG* blockers, this position is blank. Mutations of N30(39) in ChTx and AgTx2 [X(X) means the relative position in the toxin (position in ET sequence)] weakened binding to *Shaker* by 840-<sup>35</sup> and 700-fold,<sup>36</sup> respectively. The N31(39)G mutant of NTx annihilates its Kv1.3 block activity.<sup>37</sup> In contrast, the G30(39)N mutation in IbTx, a highly specific BK<sub>Ca</sub> blocker, restored a high affinity for Kv1.3.<sup>37</sup> These results strongly support that this position is a critical determinant for the pharmacological selectivity of scorpion toxins. At P05 PIC, positions 3 and 4

are identified as class-specific residues. Position 3 and 4 are occupied by two polar residues, Asp and Ser in *hERG* blockers, respectively, but blank in most other toxins. They are located on the unique long N-terminal region in *hERG* blockers, which is rich in charged residues and serines. From position 1 to 10, 3 Asp, 2 Lys, 1 Arg, and 2 Ser are present, forming a very strong hydrophilic patch.

At P07 PIC, 8 class-specific residues are identified, including positions 5, 13, 17, 23, 25, 28, 29, and 35. They are scattered throughout the whole sequence. While side-chains at position 5 and 23 are highly variable in *Shaker*/BK<sub>Ca</sub> and SK<sub>Ca</sub> blockers, they are conserved in *hERG* blockers and are Cys. They form the fourth disulfide bridge, which connects the unique long N-terminal region in *hERG* blockers to the main scaffold. In most toxins, position 35 is occupied by a buried Gly, which may contribute to toxin folding. Position 13 is often occupied by a polar and uncharged residue in *Shaker*/BK<sub>Ca</sub> blockers, such as Gly, Ser, Thr, and Asn. However, it is substituted by a charged residue Lys in *hERG* blockers and was blank in SK<sub>Ca</sub> blockers. Position 17 retains a hydrophobic residue in *hERG* blockers (Tyr) and SK<sub>Ca</sub> blockers (Leu), but is often blank in *Shaker*/BK<sub>Ca</sub> blockers. Position 25 is occupied by Lys in *hERG* blockers and Arg in SK<sub>Ca</sub> blockers. In *Shaker*/BK<sub>Ca</sub> blockers, it is often occupied by a basic residue (Lys or Arg) too. Position 28 is often occupied by a polar residue or left blank, while Position 29 is often occupied by a nonpolar residue or left blank. At P08 PIC, 3 positions, including positions 16, 40 and 42, emerge as class-specific positions. Positions 16 and 40 were aromatic residues (Tyr or Phe) in most *hERG* blockers but blank in other toxins. Position 42 mostly retains a basic residue, typically Lys. At higher PICs (P09 and P10), noises emerged precluding any further conclusions. Thus, we combined the ET residues from P01 to P08 to further study toxin binding surfaces.

Previous studies already indicated that ET residues could well overlay with the crucial residues for protein-protein docking.<sup>8</sup> This also holds true in toxin-channel interactions.<sup>38</sup> For instance, the mutagenesis works of BeKm-1 indicated that 2 basic residues (K18 and R20) in the  $\alpha$ -helix face were critical for its *hERG* block activity. Moreover, 5 other residues, including R1, Y11, F14, K23, and R27, were found to be moderately important for its activity.<sup>39</sup> Our ET analysis accurately highlights the 2

Fig. 4. Evolutionary traces for PIC P01–P10, aligned with the amino acid sequence of  $\gamma$ -KTx1.1, CnErg1. Conserved residues in ET sequences are shown and framed. Class-specific residues are denoted by X. Neutral residues are denoted by dashes. The buried residues in CnErg1 are shadowed. Position numbers above ET sequences were used throughout our analysis.

Fig. 5. ET highlighted residue clusters into two patches on opposite sides. (A) Four aromatic residues and 2 basic residues form a strong hydrophobic patch, together with 2 cations. (B) Three polar residues, including 2 charged residues, form a hydrophilic patch. (C) Proposed docking mode between CnErg1 and *hERG* channel. Y14, Y16, Y17, and F36 can tightly bind to W585 and I593 on the amphipathic  $\alpha$ -helix via the hydrophobic interaction. K38 and K13 can form the cation- $\pi$  interaction with W585. Electrostatic repulsion may occur between E575, H578 on the channel and D3, K25 on CnErg1, respectively. Pro632 may form some hydrogen bonds with the hydrophilic patch. Part of the selectivity filter (GFG) is highlighted in yellow.



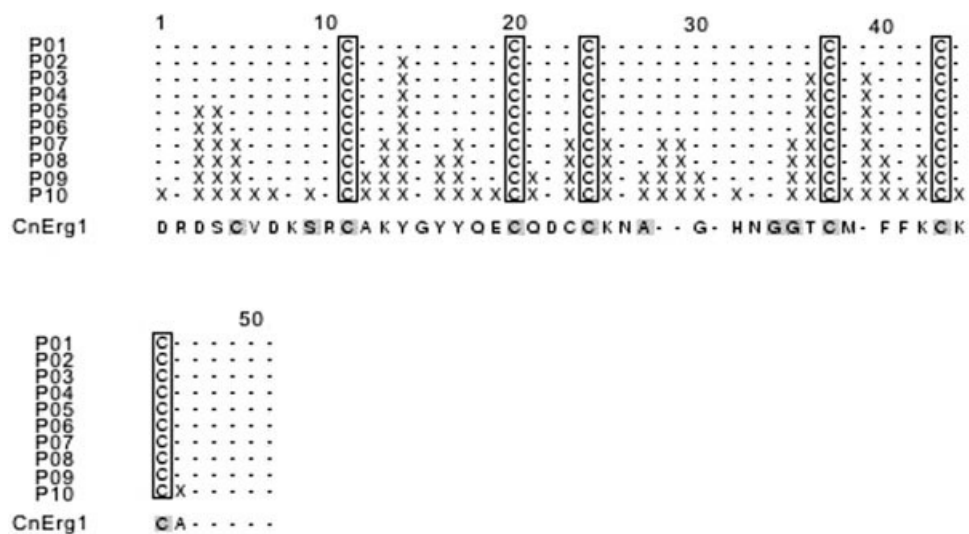


Figure 4.

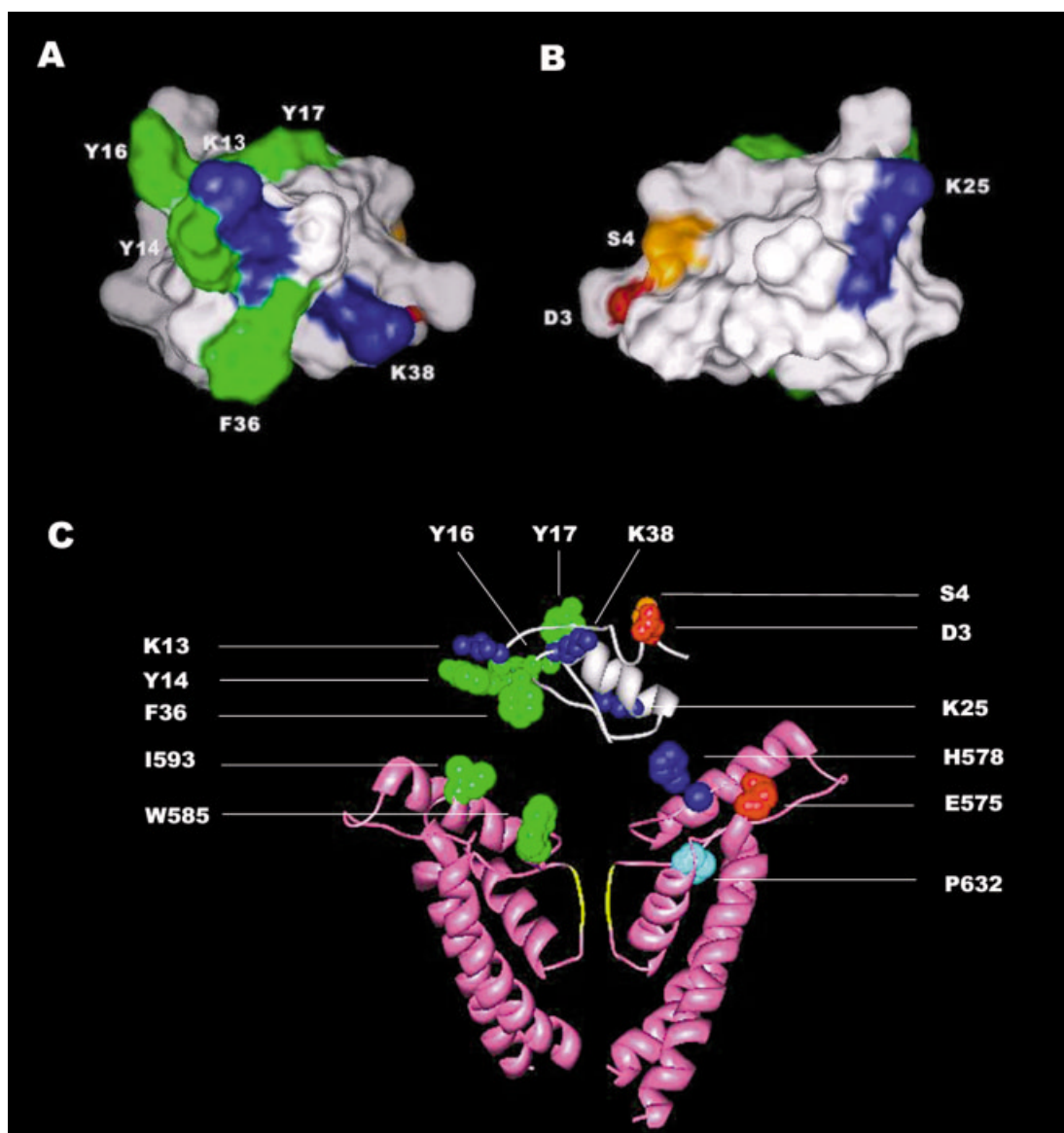


Figure 5.

crucial residues K18 and R20, as well as 3 of the 5 moderate residues. Then, using ET residues and the structure, it is possible now to study the  $\gamma$ -KTx-*hERG* binding surface.

### **CnErg1-*hERG* binding surface prediction**

Figure 5 shows the mapping of class-specific ET residues on the 3D structure of CnErg1. Four aromatic residues and 2 basic residues are clustered to one face around  $\beta$ -turns, which could form a strong hydrophobic cluster together with 2 cations [Fig. 5(A)]. On its opposite face, 3 polar residues, including 2 charged residues, were located, and they could form a hydrophilic patch [Fig. 5(B)]. The fact that D3 and S4 are in close proximity, with K25 being further away, might suggest that they interact with separate residues on *hERG* channel.

Previous studies showed that the turret region of *hERG* is crucial for CnErg1 binding.<sup>40</sup> The distinctive long turret region of *hERG* could form an amphipathic  $\alpha$ -helix with hydrophobic residues clustered to one exposed surface, which, in contrast to the pore helix and selectivity filter, are mainly involved in the binding with CnErg1.<sup>41</sup> By mutant analysis, 2 clearly hydrophobic residues (W585, I593) plus G590 and 1 residue P632 at the linker between P region and S6 helix were found to be crucial for CnErg1 binding.<sup>6</sup> However, the spacial distances among these residues are unknown, because the 3D structure of *hERG* channel is not available yet. Luckily, the crystal structure of KvAP channel from bacterial, the first crystallized voltage-gated  $K^+$  channel, has recently been reported.<sup>28</sup> KvAP has 6 transmembrane segments and shows a higher sequence homology with eukaryotic  $K^+$  channels than KcsA. Based on this novel structure, the S5-P-S6 region of *hERG* channels was modeled by the Swiss-Model server [Fig. 5(C)]. On this modeled structure, W585 and I593 are well solvent-exposed on the  $\alpha$ -helix. G590, which is slightly polar, may have a structural role and contribute in the formation of the correct amphipathic  $\alpha$ -helix conformation. P632 locates at the bottom of the outside vestibule, close to 2 charged residues, E575 and H578, whose charges were found to repulse toxin binding.<sup>6</sup>

Based on the ET-proposed functional residues of the toxin and its binding sites on the channel demonstrated by mutagenesis studies,<sup>6,31</sup> we docked CnErg1 onto the *hERG* channel briefly by the program Chimera [Fig. 5(C)]. In this proposed interaction mode, several forces are involved in the interaction. Given the fact that CnErg1 binding is only slightly influenced by extracellular pH, and that charge neutralization in the turret region has a modest or no effect on toxin binding,<sup>6</sup> electrostatic interaction should not be the main force for toxin binding. We propose that hydrophobic interactions should be the driving force: The hydrophobic patch composed of 4 aromatic residues (Y14, Y16, Y17, and F36) in CnErg1 can tightly bind to W585 and I593 on the amphipathic  $\alpha$ -helix. On the hydrophobic patch, 2 Lys residues were also highlighted by ET analysis. Recent research has shown that a wide range of cations, like protonated amines ( $RNH_3^+$ ), can form a strong interaction with the aromatic side-chain, which is called cation- $\pi$  interaction and

is comparable to or stronger than a typical hydrogen bond.<sup>42</sup> This kind of force has been found in many ligand-protein interactions, such as neurotransmitter-ligand gated ion channel, agonist-GPCR (G-protein coupled receptor), substrate-enzyme, and others.<sup>42</sup> Thus, K14 and K38 can have cation- $\pi$  interaction with W585, which is also a very strong interaction force. Thus one head of CnErg1 can bind very tightly to the external amphipathic  $\alpha$ -helix via hydrophobic and cation- $\pi$  interactions. Electrostatic interactions are much less important for CnErg1-*hERG* interaction than AgTx2-*Shaker* or P05-SK<sub>Ca</sub>, although they cannot be ruled out completely. Knowing that *hERG* mutants E575C and H578C showed a higher affinity to CnErg1 than does WT *hERG*,<sup>6</sup> electrostatic repulsion may occur between E575, H578 on the channel and D3, K25 on CnErg1, respectively. The important residue P632 may form some strong interaction with the hydrophilic patch of CnErg1, which can anchor another head of CnErg1 on the bottom of the outer vestibule.

Considering its distinctive binding region on the  $K^+$  channel, we call CnErg1 a "turret blocker" to show the difference with many  $K^+$  channel "pore blockers" such as ChTx and AgTx2.<sup>7</sup> For pore blockers, the toxin binding surface exists in the  $\beta$ -sheet region and interacts with the pore helix and selectivity filter of  $K^+$  channel. However, the turret blocker CnErg1 uses two "heads" of the structure to interact with the turret region of *hERG* channel. In most of pore blockers, Lys27 residue (ChTX numbering) in the  $\beta$ -sheet face directly plugs the selectivity filter to fully occlude the  $K^+$  pathway. The equivalent position in CnErg1 is occupied by an uncharged residue, Thr, and CnErg1 can only cover the outer vestibule of channel so that residual current can still pass through the channel.<sup>6</sup> Electrostatic force is much less important for the turret blocker binding than pore blockers, and hydrophobic interaction seems to play a key role in this binding.

A recent study by Zhang et al.<sup>31</sup> demonstrated that  $\gamma$ -KTx2.1, BeKm-1, also is a "turret blocker."<sup>31</sup> BeKm-1 and CnErg1 have a different disulfide bridging pattern and do not share any significant homology in the primary structure. However, in term of interaction with the *hERG* channel, they share similar interaction surfaces. The critical binding sites of BeKm-1 on *hERG* channel are W585, G590, Q592, and I593 on the turret region and S631, P632 on the bottom of the outside vestibule, which are almost overlapped with those of CnErg1 (W585, G590, I593, and P632). Moreover, the important functional residues of BeKm-1 (R1, Y11, F14, K18, R20, F21, K23, and R27) mainly clustered to 2 patches, 1 hydrophobic and 1 hydrophilic, and are located on the two opposite heads of the toxin molecule just like the proposed functional clusters of CnErg1.<sup>3,31,39</sup> Therefore, scorpion  $\gamma$ -KTxs seem to share the same interaction mode regardless of their different primary structures.<sup>43</sup>

In this study, we determined the NMR structure of  $\gamma$ -KTx1.1 and additionally explored critical residues for its binding to *hERG* channel. This work sheds light on the novel interaction mode between scorpion  $\gamma$ -KTx and *hERG* channel, in which the toxin is proposed to act as a turret blocker to cover the outer vestibule of the channel. [The



atomic coordinates of the structure of native CnErg1 have been deposited with RCSB PDB (PDB code: 1PX9).]

### ACKNOWLEDGMENT

The 600 MHz NMR spectrometer was funded by the Region Ile de France and the Institut Pasteur.

### REFERENCES

- Wickenden A. K(+) channels as therapeutic drug targets. *Pharmacol Ther* 2002;94:157–182.
- Tytgat J, Chandy KG, Garcia ML, Gutman GA, Martin-Eauclaire MF, van der Walt JJ, Possani LD. A unified nomenclature for short-chain peptides isolated from scorpion venoms: alpha-KTx molecular subfamilies. *Trends Pharmacol Sci* 1999;20:444–447.
- Rodriguez de la Vega RC, Merino E, Becerril B, Possani LD. Novel interactions between K<sup>+</sup> channels and scorpion toxins. *Trends Pharmacol Sci* 2003;24:222–227.
- Warmke JW, Ganetzky B. A family of potassium channel genes related to EAG in *Drosophila* and mammals. *Proc Natl Acad Sci USA* 1994;91:3438–3442.
- Curran ME, Splawski I, Timothy KW, Vincent GM, Green ED, Keating MT. A molecular basis for cardiac arrhythmia: *HERG* mutations cause long QT syndrome. *Cell* 1995;80:795–803.
- Pardo-Lopez L, Zhang M, Liu J, Jiang M, Possani LD, Tseng GN. Mapping the binding site of a human ether-a-go-go-related gene-specific peptide toxin (ErgTx) to the channel's outer vestibule. *J Biol Chem* 2002;277:16403–16411.
- Xu CQ, Zhu SY, Chi CW, Tytgat J. Turret and pore blocker of K<sup>+</sup> channels: what is the difference? *Trends Pharmacol Sci* 2003;24:446–448.
- Yao H, Kristensen DM, Mihalek I, Sowa M E, Shaw C, Kimmel M, Kavraki L, Lichtarge O. An accurate, sensitive, and scalable method to identify functional sites in protein structures. *J Mol Biol* 2003;326:255–261.
- Torres AM, Bansal P, Alewood PF, Bursill JA, Kuchel PW, Vandenberg JI. Solution structure of CnErg1 (ergtoxin), a *HERG* specific scorpion toxin. *FEBS Lett* 2003;539:138–142.
- Pritchard L, Dufton MJ. Evolutionary trace analysis of the Kunitz/BPTI family of proteins: functional divergence may have been based on conformational adjustment. *J Mol Biol* 1999;285:1589–1607.
- Innis CA, Shi J, Blundell TL. Evolutionary trace analysis of TGF-beta and related growth factors: implications for site-directed mutagenesis. *Protein Eng* 2000;13:839–847.
- Aloy P, Querol E, Aviles FX, Sternberg MJ. Automated structure-based prediction of functional sites in proteins: applications to assessing the validity of inheriting protein function from homology in genome annotation and to protein docking. *J Mol Biol* 2001;311:395–408.
- Lichtarge O, Bourne HR, Cohen FE. An evolutionary trace method defines binding surfaces common to protein families. *J Mol Biol* 1996;257:342–358.
- Gurrola GB, Rosati B, Rocchetti M, Pimienta G, Zaza A, Arcangeli A, Olivetto M, Possani LD, Wanke E. A toxin to nervous, cardiac, and endocrine *ERG* K<sup>+</sup> channels isolated from *Centruroides noxius* scorpion venom. *FASEB J* 1999;13:953–962.
- Scaloni A, Bottiglieri C, Ferrara L, Corona M, Gurrola GB, Batista C, Wanke E, Possani LD. Disulfide bridges of ergtoxin, a member of a new sub-family of peptide blockers of the ether-a-go-go-related K<sup>+</sup> channel. *FEBS Lett* 2000;479:156–157.
- Kupce E, Keifer PA, Delepierre, M. Adiabatic TOCSY MAS in liquids. *J Magn Reson* 2001;148:115–120.
- Kumar A, Ernst RR, Wüthrich K. A two-dimensional nuclear Overhauser enhancement (2D NOE) experiment for the elucidation of complete proton-proton cross-relaxation networks in biological macromolecules. *Biochem Biophys Res Commun* 1980;95:1–6.
- Aue WP, Bartholi E, Ernst RR. Two-dimensional spectroscopy: application to nuclear magnetic resonance. *J Chem Phys* 1976;64:2229–2246.
- Boyd J, Dobson CM, Redfield C. Correlation of proton chemical shifts in proteins using two-dimensional double-quantum spectroscopy. *J Magn Reson* 1983;55:170–176.
- Braunschweiler L, Ernst RR. Coherence transfer by isotropic mixing: application to proton correlation spectroscopy. *J Magn Reson* 1983;53:521–528.
- Piotto M, Saudek V, Sklenar V. Gradient-tailored excitation for single-quantum NMR spectroscopy of aqueous solutions. *J Biomol NMR* 1992;2:661–665.
- Wüthrich K. NMR of proteins and nucleic acids. New York: Wiley; 1986.
- Bartels C, Xia T-H, Billeter M, Güntert P, Wüthrich K. The program XEASY for computer-supported NMR spectral analysis of biological macromolecules. *J Biomol NMR* 1995;5:1–10.
- Nilges M, Macias MJ, O'Donoghue SI, Oschkinat H. Automated NOESY interpretation with ambiguous distance restraints: the refined NMR solution structure of the pleckstrin homology domain from beta-spectrin. *J Mol Biol* 1997;269:408–422.
- Linge JP, O'Donoghue SI, Nilges M. Automated assignment of ambiguous nuclear overhauser effects with ARIA. *Methods Enzymol* 2001;339:71–90.
- Brünger AT, Adams PD, Clore GM, DeLano WL, Gros P, Gross-Kunstleve RW, Jiang JS, Kuszewski J, Nilges M, Pannu NS, Read RJ, Rice LM, Simonson T, Warren GL. Crystallography & NMR System: a new software suite for macromolecular structure determination. *Acta Crystallogr D Biol Crystallogr* 1998;54:905–921.
- Linge JP, Habeck M, Rieping W, Nilges M. ARIA: automated NOE assignment and NMR structure calculation. *Bioinformatics* 2003;19:315–316.
- Jiang Y, Lee A, Chen J, Ruta V, Cadene M, Chait BT, MacKinnon R. X-ray structure of a voltage-dependent K<sup>+</sup> channel. *Nature* 2003;423:33–41.
- Peitsch MC, Schwede T, Guex N. Automated protein modelling—the proteome in 3D. *Pharmacogenomics* 2000;1:257–266.
- Corona M, Gurrola GB, Merino E, Cassulini RR, Valdez-Cruz NA, Garcia B, Ramirez-Dominguez ME, Coronas FL, Zamudio FZ, Wanke E, Possani LD. A large number of novel ergtoxin-like genes and *ERG* K<sup>+</sup>-channels blocking peptides from scorpions of the genus *Centruroides*. *FEBS Lett* 2002;532:121–126.
- Zhang M, Korolkova YV, Liu J, Jiang M, Grishin EV, Tseng GN. BeKm-1 is a *hERG*-specific toxin that shares the structure with ChTx but the mechanism of action with ErgTx1. *Biophys J* 2003;84:3022–3036.
- Shakkottai VG, Regaya I, Wulff H, Fajloun Z, Tomita H, Fathallah M, Cahalan MD, Gargus JJ, Sabatier JM, Chandy KG. Design and characterization of a highly selective peptide inhibitor of the small conductance calcium-activated K<sup>+</sup> channel, SkCa2. *J Biol Chem* 2001;276:43145–43151.
- Possani LD, Selisko B, Gurrola GB. Structure and function of scorpion toxins affecting K<sup>+</sup>-channels. *Perspectives Drug Disc Des* 1999;15/16:15–40.
- Garcia ML, Gao Y, McManus OB, Kaczorowski GJ. Potassium channels: from scorpion venoms to high-resolution structure. *Toxicon* 2001;39:739–748.
- Goldstein SA, Pheasant DJ, Miller C. The charybdotoxin receptor of a *Shaker* K<sup>+</sup> channel: peptide and channel residues mediating molecular recognition. *Neuron* 1994;12:1377–1388.
- Ranganathan R, Lewis JH, MacKinnon R. Spatial localization of the K<sup>+</sup> channel selectivity filter by mutant cycle-based structure analysis. *Neuron* 1996;16:131–139.
- Schroeder N, Mullmann TJ, Schmalhofer WA, Gao YD, Garcia ML, Giangiacomo KM. Glycine 30 in ibertoxin is a critical determinant of its specificity for maxi-K versus K(V) channels. *FEBS Lett* 2002;527:298–302.
- Zhu S, Isabelle H, Dyason K, Verdonck F, Tytgat J, Huys I. Evolutionary trace analysis of scorpion toxins specific for K-channels. *Proteins* 2004;54:361–370.
- Korolkova YV, Bocharov EV, Angelo K, Maslennikov IV, Grinenko OV, Lipkin AV, Nosyreva ED, Pluzhnikov KA, Olesen SP, Arseniev AS, Grishin EV. New binding site on common molecular scaffold provides *HERG* channel specificity of scorpion toxin BeKm-1. *J Biol Chem* 2002;277:43104–43109.
- Pardo-Lopez L, Garcia-Valdes J, Gurrola GB, Robertson GA, Possani LD. Mapping the receptor site for ergtoxin, a specific blocker of *ERG* channels. *FEBS Lett* 2002;510:45–49.
- Liu J, Zhang M, Jiang M, Tseng GN. Structural and functional role of the extracellular s5-p linker in the *HERG* potassium channel. *J Gen Physiol* 2002;120:723–737.
- Zacharias N, Dougherty DA. Cation- $\pi$  interactions in ligand recognition and catalysis. *Trends Pharmacol Sci* 2002;23:281–287.
- Possani LD, Rodriguez de la Vega, RC. Response to Xu et al.: hypothesis-driven science paves the way for new discoveries. *Trends Pharmacol Sci* 2003;24:448–449.